

Gravity anomaly patterns in the south-central Zimbabwe Archaean craton and their geological interpretation

R.T. Ranganai^{a,*}, K.A. Whaler^{b,1}, C.J. Ebinger^{b,2}

^aDepartment of Physics, University of Zimbabwe, P.O. Box MP167, Mt. Pleasant, Harare, Zimbabwe

^bDepartment of Earth Sciences, University of Leeds, Leeds LS2 9JT, England, UK

Received 15 May 2007; received in revised form 24 January 2008; accepted 29 January 2008

Abstract

The granite-greenstone terrain of south-central Zimbabwe, encompassing the Belingwe (Mberengwa) greenstone belt and sections of the Great Dyke, provides important constraints on models for the evolution of the Zimbabwe craton and the Archaean crust in general. In this paper we enhance and model existing and recently acquired gravity data from the region and correlate the anomalies and their derivatives with the known basement geology to evaluate models for greenstone belt development. We also study the spatial gneiss-granite-greenstone association in general, and the geologic implications of models of the anomaly patterns in particular. Although the Belingwe greenstone belt has been mapped, its subsurface geometry is poorly known. Similarly, the Great Dyke is well studied, but no systematic study of the extent and cross-cutting relations of other mafic dykes in the Archaean crust has been undertaken.

The regional gravity field shows no evidence for crustal thickness variations in the area and the gravity anomalies can be explained by lateral density variations of the supracrustal rocks. Prominent gravity highs are observed over the high density ($\leq 3000 \text{ kg/m}^3$) volcano-sedimentary piles (greenstone belts) and ultramafic complexes. Well-defined elongate, sub-oval/elliptical gravity lows are associated with intrusive granitic plutons. The granite-greenstone contacts are marked by steep gravity gradients of up to 5 mGal/km that imply steeply dipping or near-vertical contacts for the anomalous bodies. This is tested and confirmed by $2^{1/2}$ D modelling of gravity profiles across the Belingwe and Fort Rixon greenstone belts, constrained by measured densities and observed geological data. The modelling also indicates that these belts, and possibly all the belts in the study area (based on comparable densities and anomaly amplitudes), have limited depth extents in the range of 3–5 km. This is comparable to thicknesses obtained elsewhere from deep seismic reflection data and geoelectrical studies, but mapped stratigraphic thicknesses give a maximum depth extent of about 9.5 km. Present studies and previous work support the idea that the volcanics were extruded within rift zones and laid on older granitic crust, followed by subsidence and rapid deposition of sediments that were sourced from the adjacent basement terrains. The volcano-sedimentary sequences were subsequently deformed by intruding younger plutons and affected by late-stage strike-slip activity producing cross-cutting structures.

© 2008 Elsevier Ltd. All rights reserved.

Keywords: Archaean crust; Zimbabwe craton; Greenstone belt; Gravity modelling; Depth extent; Autochthonous origin

1. Introduction

Parts of the southeastern region of the Archaean Zimbabwe craton (Fig. 1) have been used as examples of gneiss-granite-greenstone type areas for the rest of the craton (Wilson et al., 1978; Wilson, 1979, 1981), and even the Archaean in general (e.g., Condie, 1981; Nisbet, 1987). The region also hosts various mineral deposits, with a few operating mines producing economically significant amounts of gold, asbestos, emeralds, nickel and chromite,

* Corresponding author. Present address: Department of Physics, University of Botswana, P. Bag UB0704, Gaborone, Botswana. Tel: +267 3552465; fax: +267 3185097.

E-mail address: ranganai@mopipi.ub.bw (R.T. Ranganai).

¹ Present address: School of GeoSciences, University of Edinburgh, Grant Institute, West Mains Road, Edinburgh EH9 3JW, UK.

² Present address: Department of Geology and Geophysics, Royal Holloway, England, UK.

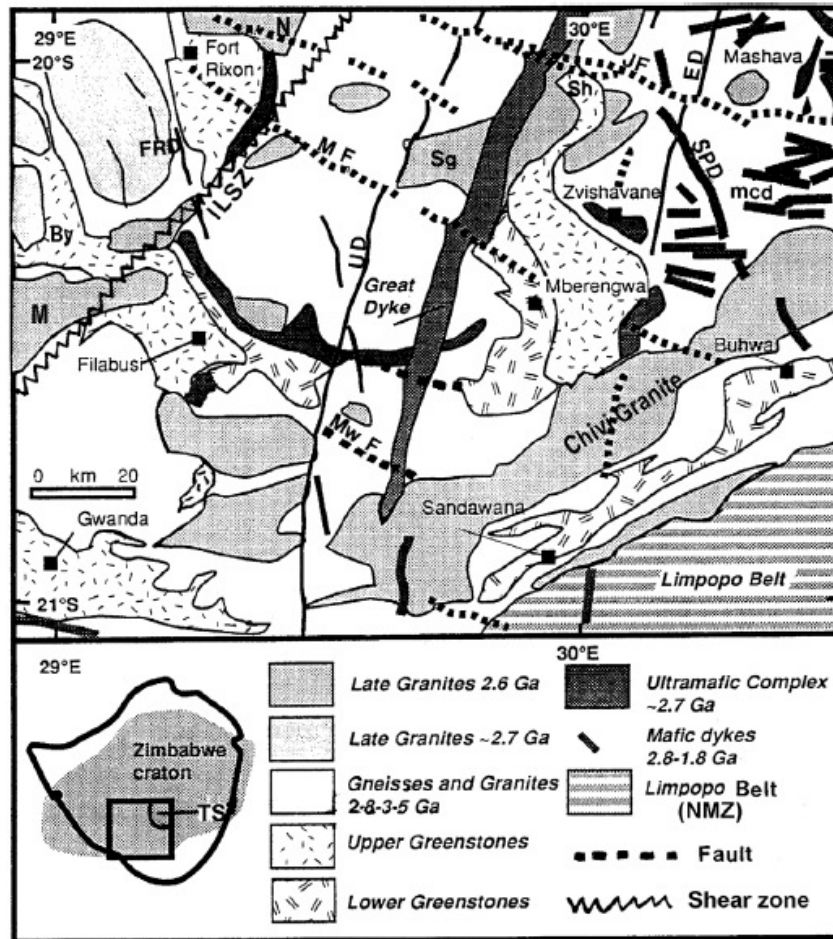


Fig. 1. Simplified geological map of the south-central Zimbabwe Archaean craton. Geological units and features labelled are: By = Bulawayo, MwF = Mwenzi fault; MF = Mtshinge fault, JF = Jenya fault, SPD = Sebanga Poort Dyke, ED = East dyke; MCD = Mashava-Chivi dykes; M = Mbalabala granite; N = Nalatale granite; Sh = Snake head section; FRD = Fort Rixon dykes; UD = Umvimeela dyke, Sg = Shabani granite, ILSZ = Irrisvale-Lanchaster shear zone. Inset: TS = Tokwe segment of Wilson (1979, 1990), the 3.5 Ga Gneiss Complex represents the oldest crustal segment of the country.

within and near the greenstone belts. Most of the geological units have, therefore, been studied extensively by geological methods (e.g., Bickle and Nisbet, 1993 and references therein), but the subsurface geometry and regional tectonic context of these remain unresolved. Despite its tectonic and economic importance, the area has not received systematic regional geophysical interpretation and little is known of the subsurface geometry of granite-greenstone contacts at depth. Gravity data offer a valuable insight to bedrock geology obscured beneath surficial cover and inherently contain information on the configuration of

rock formations at depth but they cannot, on their own, be uniquely interpreted and require geological and physical property constraints. In this study, gravity data from 485 new stations are combined with those from 865 previously surveyed stations and 87 new density measurements to produce a detailed Bouguer gravity map of the area.

The main objective of the paper is to correlate gravity anomalies and their derivatives with the known basement geology, and investigate the subsurface geological structure. We use cross-cutting relationships to investigate the spatial and temporal relationships between the greenstone

successions and the surrounding granitoids, including their mode of emplacement. The aims are achieved by analysing the data using potential field transformations and interpretation techniques, and forward modelling constrained by measured rock densities and observed geologic data. These new constraints on the subsurface geometry of the Belingwe region are used to evaluate tectonic models of greenstone belts.

2. Tectonic setting

The Archaean Zimbabwe craton contains some of the oldest known fragments of the Earth's Precambrian crust. It consists of folded volcano-sedimentary successions of greenstone belts, the associated areally extensive gneisses and granites (3.5–2.6 Ga), the Great Dyke (2.46 Ga), and layered ultramafic intrusions and mafic dyke swarms of various ages (Wilson, 1981; Fig. 1). The greenstone stratigraphy is divided into the Sebakwian (3.5 Ga), the Bulawayan, and Shamvaian (2.7 Ga) Groups, with the Bulawayan further subdivided into the Lower Greenstones (~2.9 Ga) and the Upper Greenstones (2.7 Ga), which are separated by an unconformity (Wilson et al., 1978; Wilson, 1979, 1981; Taylor et al., 1991). A more recent revision of the stratigraphy of the Archaean greenstone belts is presented by Wilson et al. (1995) while Blenkinsop et al. (1997) provide an overview of the structure and tectonics of the craton. The NE-trending Neoproterozoic Limpopo orogenic belt of high-grade gneisses and granulites separates the Zimbabwe craton from the Kaapvaal craton in the south.

Major geological units in the study area include the Belingwe (Mberengwa), Buhwa, Bulawayo, Filabusi, Fort Rixon and Gwanda greenstone belts, 'young' K-rich granites (e.g., Chivi Granite) and sections of the Great Dyke and its satellites (East and Umvimeela dykes), set within ancient tonalitic gneisses (Fig. 1). The main greenstone belts have suffered at least three phases of deformation and have been folded into 'simple synclinal' form perhaps due to the intrusion of the 'young'/late Granites (Wilson, 1979, 1981; Campbell et al., 1992; Blenkinsop et al., 1997). Several layered ultramafic intrusions (~2.8 Ga Mashava Ultramafic Suite, Wilson, 1979) are scattered throughout the area and are hosts to large asbestos mines at Mashava and Zvishavane (Fig. 1). Mafic dyke swarms of Archaean (2.8 Ga) and Proterozoic (2.0–1.8 Ga) age occur east of the Belingwe belt and west and south of the Fort Rixon belt, respectively (Wilson et al., 1987). The swarm constituting the Mashava-Chivi dykes (MCD, Fig. 1) are considered, together with the associated Mashava Ultramafic Suite, to be part of the feeder system to basaltic lavas of the 2.7 Ga Upper Greenstones which dominate the greenstone succession (Wilson, 1979, 1990; Wilson et al., 1987).

Of the units in the area, only the Belingwe belt is geologically and geophysically well studied (e.g., Martin, 1978; Ranganai, 1985, 1993; Bickle and Nisbet, 1993). It contains the most complete greenstone sequences in the craton, and

its well preserved and exposed stratigraphy has been correlated with units across much of the craton (Wilson et al., 1978, 1995; Wilson, 1979; Taylor et al., 1991). There are two distinct greenstone sequences: the ~2.9 Ga Mtshingwe Group (Lower Greenstones) of peridotitic and basaltic komatiites and clastic sediments, which is unconformably overlain by the 2.7 Ga Ngezi Group (Upper Greenstones) composed of conglomerates, peridotitic and basaltic komatiites and thick sequences of tholeiites and andesites, capped by a thin layer of shallow-water clastic sediments and carbonates (Bickle and Nisbet, 1993). The Ngezi Group was deposited unconformably on an irregular terrain of Mtshingwe Group, gneiss and tonalite, and there is strong evidence of an unconformity between the latter and older granite-greenstone basement (Bickle et al., 1975; Blenkinsop et al., 1993).

The Belingwe belt has been cited as a typical example of an autochthonous relation between greenstones and continental basement (Bickle et al., 1975, 1994; Nisbet, 1987; Blenkinsop et al., 1993, 1997; Hunter et al., 1998), but a few workers present an allochthonous interpretation for the ~6 km thick basalt/komatiite pile with respect to the thin basal sedimentary sequence lying unconformably on the gneisses (e.g., Kusky and Kidd, 1992; Kusky and Winsky, 1995). The former group argues that the greenstone rocks were originally deposited in a rift basin on weak lithosphere that underwent deformation from the weight of the lavas, thereby explaining the localized distribution of greenstones (see Bickle and Nisbet, 1993). On the other hand, Kusky and Kidd's model of allochthonous imbrication implies significant, broadly unidirectional transport of the over-riding sheet (the "Mberengwa Allochthon") for probably >28 km (Campbell and Pitfield, 1994). A simple 2D gravity model using limited data on the belt yielded a ~7 km thick basin-like structure supportive of the "granite basement" idea (Ranganai, 1985), but does not rule out the alternative model. Another possible tectonic environment mentioned is a magmatic arc for the western succession of the Upper Greenstones (Wilson, 1981; Nisbet et al., 1981), but this has been challenged by Wilson et al. (1995) as too simplistic. In other Archaean terrains, popular models invoke sea-floor spreading and subduction, obduction of oceanic plateaus, and subduction-driven terrane accretion (e.g., Card, 1990; de Wit et al., 1992; Windley, 1993; Myers, 1995; De Wit and Ashwal, 1997a).

With the exception of Buhwa, all the other belts have lithostratigraphic sequences similar to Belingwe: ultramafic, mafic, felsic and volcano-sedimentary assemblages. The Buhwa belt is largely composed of quartzite, pelite, banded iron formation and ultramafic schists, all belonging to the 2.9 Ga Lower Greenstones or older greenstone sequence (Rollinson, 1993; Fedo et al., 1995). The anomalous stratigraphy is interpreted by Rollinson (1993) as evidence for an allochthonous origin for the Buhwa belt, as well as the Matsitama on the southwestern edge of the craton in northeast Botswana. More recently, the Buhwa belt has been interpreted as a stable shelf-succession (Fedo and

Errikson, 1996), containing a western shelf-succeSSION and an eastern deeper-water basinal facies association.

The study area is bounded to the southeast by the North Marginal Zone (NMZ) of the Limpopo Belt (LB), which consists mainly of reworked Archaean granitoid-greenstone rocks at granulite facies (Hickman, 1978; Barton and Key, 1981; van Reenen et al., 1992). The granulite rocks contain several inclusions of greenstone belt remnants, metabasites, mafic dykes, ultramafics and magnetite quartzites/banded iron formation, as narrow layers several kilometres long (Rollinson and Blenkinsop, 1995). The boundary between the NMZ and the Zimbabwe craton is marked by a southerly dipping thrust and a series of mylonite zones (Coward et al., 1976; Mkweli et al., 1995; Rollinson and Blenkinsop, 1995). This is intruded by 2.6 Ga porphyritic granite plutons whose equivalents in the craton

are the Chilimanzi granites (Robertson, 1973, 1974; Mkweli et al., 1995; Frei et al., 1999). The Limpopo orogenic belt has been a subject of a number of geophysical investigations and the Zimbabwe portion is essentially characterized by crustal thinning in a southerly direction (34 km for NMZ and 30 km for CZ) and an associated regional gravity high interpreted largely in terms of Mesozoic crustal thinning related to the breakup of Gondwana (Stuart and Zengeni, 1987; Gwavava et al., 1992, 1996).

Due to the large density contrasts between metamorphosed volcanic rocks and granites, as well as high-grade granulite rocks, gravity methods are an obvious means of mapping granite-greenstone terrains (Subrahmanyam and Verma, 1981; Reeves, 1989). Gravity and magnetic methods cannot reveal the true shape of the greenstone bodies beneath the broad basins, but can be used to place

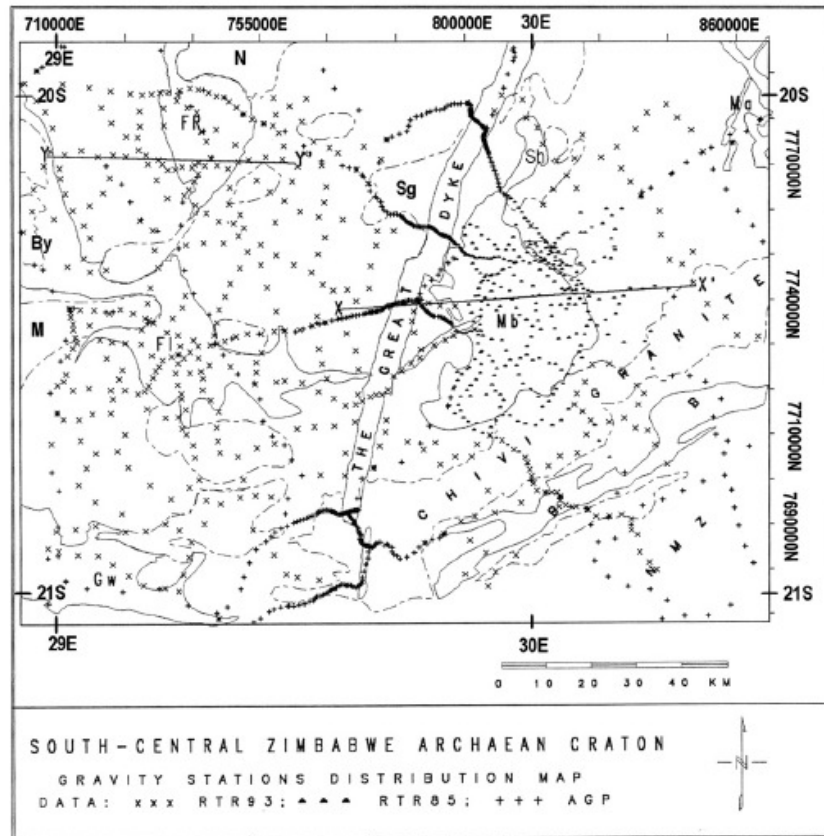


Fig. 2. Gravity station distribution map of the study area: UTM projection, zone 35S. Outlines of greenstone belts and granite plutons (dashed lines) are shown. Location of modeled gravity profiles XX' and YY' (Figs. 10 and 11) are shown. Gravity stations: RTR93 = RT Ranganai data collected in 1993 (this study); RTR85 = RT Ranganai data collected in 1985; AGP = African Gravity Project compilation/data set. Geological features labelled are greenstone belts: B = Bulwa, Fl = Filabusi, FR = Fort Rixon, Gw = Gwanda, Mb = Mberengwa; other units: Ma = Mashava ultramafic complex; NMZ = North marginal zone of Limpopo belt. Note the detailed traverses across the Great Dyke and the greenstone belts.

bounds on their thickness and nature of side contacts. Gravity and density measurements which form the basis of this study are briefly described below. An associated study of aeromagnetic data provides additional support for the gravity models (Ranganai, 1995).

3. Gravity data

The existing 865 gravity data points from the African Gravity Project (AGP) data base (Fairhead et al., 1988) were considered inadequate for the study of the configuration of the greenstone belts and the regional crustal structure of the area as most of them come from traverses across the Great Dyke and the Belingwe greenstone belt (Fig. 2). A fieldwork programme was therefore undertaken in 1993 to establish detailed gravity traverses at 1–3 km spacing across the Filabusi, Fort Rixon and Buhwa greenstone belts and the Chivi granite (Fig. 2). A regional (3–6 km spacing) network of stations over the belts and surrounding granitoids was also acquired in order to improve the general data distribution. A LaCoste & Romberg geodetic gravimeter from the Zimbabwe Geological Survey was used along roads and motorable tracks in the area. The same instrument was also used in previous surveys which form the major part of the AGP data base for Zimbabwe (e.g., Podmore, 1985; Ranganai, 1985; Gwavava, 1990), thus making a direct link between the surveys. A network of primary base stations tied to the IGSN71 fundamental points had been previously established throughout the country and therefore adequate base stations existed in the area (Fisk and Hawadi, 1996). Several bench marks and other old stations were re-occupied to better tie the new and old surveys together.

It was possible to fix the lateral station position to ± 50 m from 1:50,000 topographic maps, sometimes aided by vehicle odometer readings. A compass was used in more difficult situations to assist in the location of stations using bearings of hills and other physical features. In exceptional cases, it was necessary to employ autonomous GPS positioning techniques. Station elevations were determined by barometric leap-frogging, controlled by trigonometric beacons, bench marks and differential GPS (DGPS) points (relative to trigonometric beacons) at approximately 10 km intervals. The terrain in the survey area is not very rugged and there were no severe weather variations, which permits confidence in the accuracy of the barometer survey. Traverses from barometric levelling were joined to make a network of closed loops whose misclosures were adjusted by a least squares program (Gwavava, 1990), with the DGPS stations, bench marks and trigonometric beacons as control points. The standard error of an adjusted height difference of unit weight was found to be 1.30 m for the network as a whole (Ranganai, 1995). The adjusted node heights and the adjustments were used to calculate individual heights along traverses. The estimated standard error of the 1993 station heights is ± 1.5 m.

Tidal and instrument drift, latitude, and elevation corrections were applied to the observed gravity readings. The corrected observed gravity values were reduced to Bouguer gravity anomalies using the GRS67 formula (Moritz, 1984) and a crustal density of 2670 kg/m^3 , and are considered accurate to less than ± 2.0 mGal, owing largely to errors in absolute height. Terrain corrections were not applied as these had been found to be < 2 mGal in previous surveys (e.g., Ranganai, 1985; Gwavava et al., 1992), compared to the ~ 40 mGal anomalies. The new 485 measurements and the existing 865 AGP data points were used to compute a simple Bouguer gravity anomaly map of the area. The ‘randomly’ distributed data were gridded at 3 km cell size in the UTM co-ordinate system using a program based on the minimum curvature technique (Smith and Wessel, 1990). They were then contoured at an interval of 2 mGal (Fig. 3).

4. Rock densities

In both gravity and magnetic modelling, known geological and physical property control reduces the non-uniqueness common in these methods. Over 80 hand samples were collected from outcrops in the vicinity of the gravity stations and their densities were determined by the traditional wet and dry method (e.g., Subrahmanyam and Verma, 1981). The rocks were thoroughly cleaned before measuring their mass both in air and totally immersed in water. A total of 87 dry density determinations were made and these were combined with those determined previously (e.g., Ranganai, 1985; Podmore, 1985). A summary of the combined rock densities is presented in Table 1 and Fig. 4. Due to the low porosity and permeability of igneous rocks involved, the determined densities are considered to closely approximate the field values (Subrahmanyam and Verma, 1981 and references therein). The influence of porosity and vesicles on density in, for example, volcanic rocks is usually less than one per cent (Henkel, 1976). Low density values from granites may be due to weathered samples (Ranganai, 1995). The apparently wide range in the ‘greenstone’ densities is due to lower values from included ultramafic schists, felsic volcanics and some amphibolites, mostly from the patchy Lower Greenstones (Henkel, 1976; cf. Ranganai, 1985, 1995). However, the uncertainties imposed by this intra-unit density variation are considered minimal and acceptable as discussed below for profile modelling. The Great Dyke values have been divided into a hybrid unit comprising serpentinized dunite, pyroxenite, gabbro-norite, harzburgite and dunite and a ‘dyke’ feeder of dunite only (cf. Podmore and Wilson, 1987).

5. Data processing

The separation of *regional* and *residual* anomalies is traditionally one of the most difficult (e.g., Gupta and Ramani, 1980), but essential parts of potential field interpretation

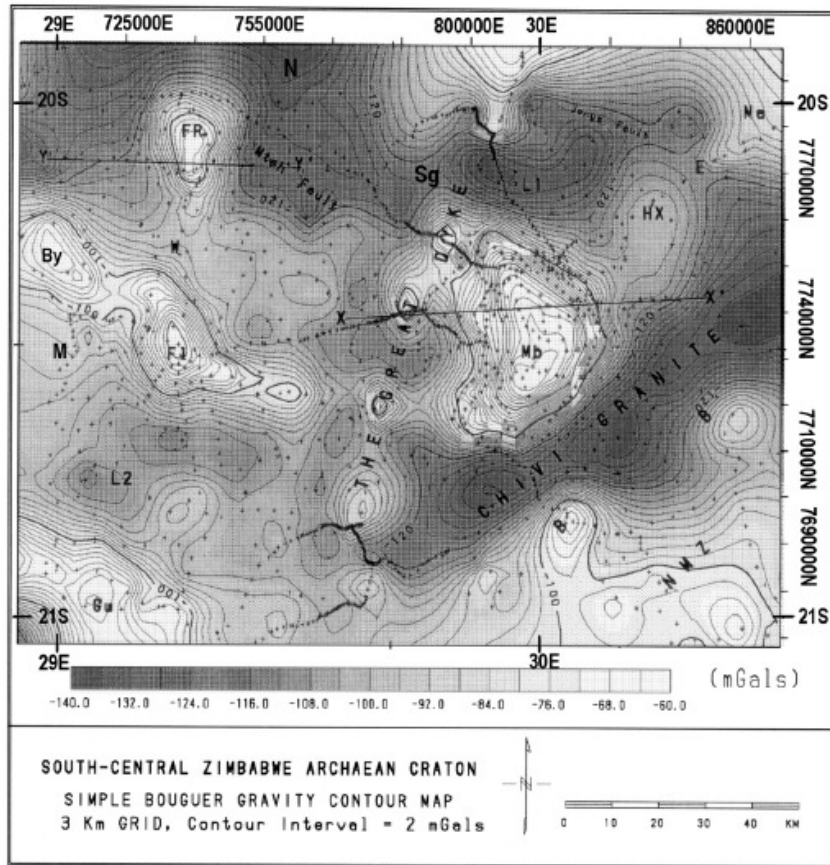


Fig. 3. Bouguer gravity anomaly and contour map (contour interval 2mGals; grey scale: dark = low, white = high). Gravity station distribution and location of modelled profiles XX' and YY' (Figs. 10 and 11) are shown. Greenstone belts and granites labelled mainly for reference purposes, but note the granite-greenstone contacts marked by steep gravity gradients (high contour density). Labels for geological units as in Figs. 1 and 2; gravity anomalies L1, L2, HX, W-E are discussed in text.

Table 1
Densities of major rock types of the granite-greenstone terrain and the Great Dyke, south-central Zimbabwe Archaean craton

Rock unit and/or rock type	Total samples	Range (kg/m ³)	Mean (kg/m ³)	Std. dev.
Granites/gneisses	46	2500–2750	2630	32
Basalts/volcanics	57	2760–398	2976	54
Ultramafics/schists	19	2725–2940	2840	20
Dolerites/dionites	15	2876–3064	3000	19
Sand/siltstones	13	2150–2670	2520	40
Great Dyke (Top) ^a	389	2830–3350	3100	29
(Feeder) ^a	26	2948–3350	3310	38

^a The Great Dyke values have been divided into a hybrid unit comprising serpentinitized dunite, pyroxenite, gabbro-norite, harzburgite and dunite for the top section and a 'dyke' feeder of dunite only (cf. Podmore and Wilson, 1987).

and a number of techniques are available including graphical and/or visual methods, wavelength filtering, spectral analysis, and upward continuation (see Blakely, 1995). Telford et al. (1990) suggested that this regional-residual separation is best achieved after examination of all other derived maps since these help determine the residual anomalies. The generally uniform Bouguer gravity values over the gneisses and tonalites in the study area suggest that a relatively uniform regional gravity field can be approximated by a zero or first order polynomial surface. A simple 'isostatic' regional (Simpson et al., 1986 and references therein) was computed by upward continuing the Bouguer gravity grid to 35 km (average crustal thickness; Stuart and Zengeni, 1987), resulting in a grid with a small range of –105 to –115 mGal, and a mean of about –109 mGal

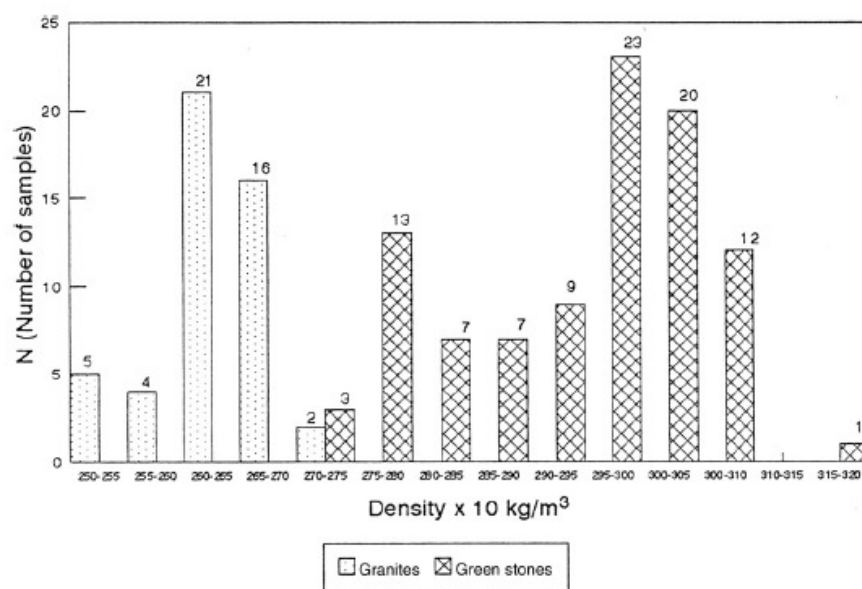


Fig. 4. Density histogram for rocks from Mberengwa (Belingwe), Filabusi and Fort Rixon. The number at the top of each column refers to the number of samples. Mean density values used for the gravity modelling of the granites and greenstones are 2630 and 2960 kg/m³, respectively.

(Ranganai, 1995). Therefore, a residual gravity map (Fig. 5) obtained by subtracting -110 mGal from the Bouguer gravity grid, as well as the derived maps discussed below, were prepared to enhance the short wavelength features that usually correspond to the supracrustal geology.

Transformations of potential field data are often helpful for general qualitative as well as quantitative interpretation. In this study, the processes applied, and products used, include apparent density mapping (Gupta and Grant, 1985), and vertical and horizontal gradients (e.g., Fig. 6). Horizontal and vertical gradients enhance short wavelength anomalies while suppressing long wavelength components caused by deep-seated features, allowing more accurate lithological contact and edge detection. This is particularly useful in determining the existence and location of steeply dipping boundaries of igneous intrusive bodies in the crystalline basement such as in the study area (e.g., Rudman et al., 1971; Thurston and Brown, 1994).

In apparent density mapping, the sources of the continuous potential field are modelled as an approximation to the distribution of density in the ground, based on the assumption that the bedrock density varies laterally but not vertically to a certain depth (Gupta and Grant, 1985). Based on measured densities and the estimated depth extent of the major units (e.g., Belingwe greenstone belt, Ranganai, 1985), this average depth extent of the supracrustal rocks was set at 6 km. The results are mean values obtained by taking grid windows covering the units under consideration. The process is applied to residual

gravity data and provides a good qualitative picture of the actual density distribution of the rocks (Gupta and Grant, 1985). The resulting average (apparent) densities of all the rocks can then be compared with the values from rock-sample measurements (Table 1).

6. Description and correlation of anomalies with geology

With regional geological mapping as the main focus, we correlate geologic trends and rock units with anomaly trends and character. Because not all processed maps can be shown, we have decided to use those products which best reflect the various characteristics of the near-surface geology of the area.

6.1. Bouguer and residual gravity maps

The calculated linear regional of -110 mGal is close to the minima of the Bouguer gravity anomalies for the greenstones, resulting in positive residual anomalies throughout these units, and in negative anomalies over the late granite plutons, in accordance with their measured densities (Table 1 and Fig. 4). The Bouguer and residual gravity maps (Figs. 3 and 5) both outline the gross aspects of the geology, but the latter has better resolution and is more closely related to the near-surface geology than the former. The two maps display several well defined gravity highs and lows of varying dimensions and relief, with anomalies of up to -60 and -140 mGal, respectively, relative to a back-

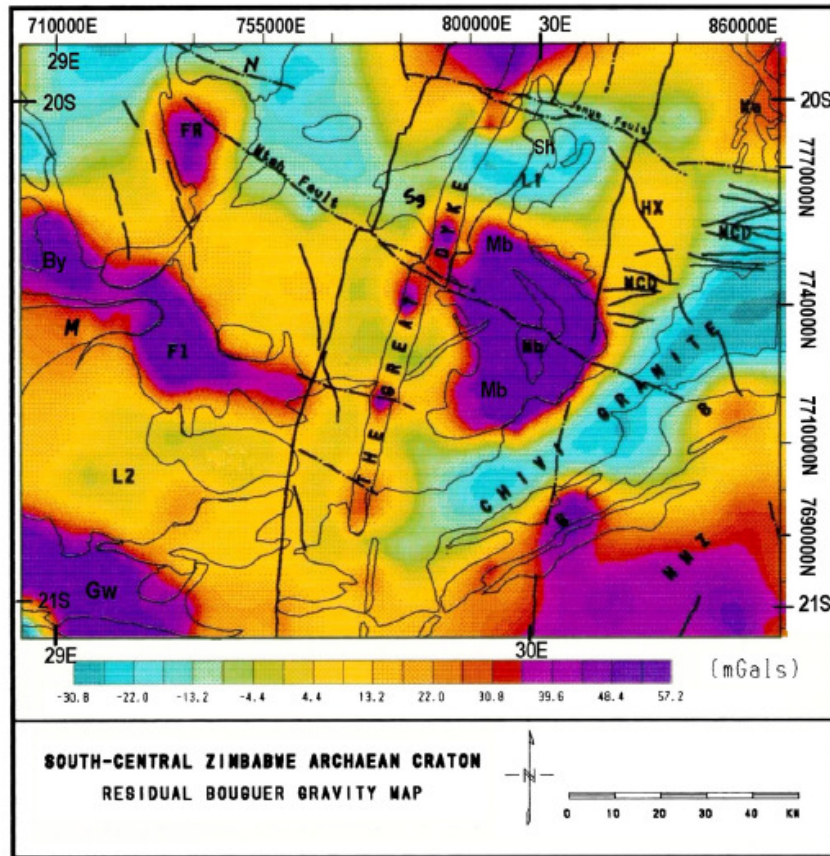


Fig. 5. Residual gravity map obtained by subtracting a mean regional of -110 mGal from the simple Bouguer gravity values. The mean was determined by upward continuation of Bouguer gravity values to 35 km, the average crustal thickness in the study area based on seismic studies of Stuart and Zengeni (1987). Labels for geological units as in Figs. 1 and 2.

ground of about -110 mGal. The high density greenstone belts (B, By, Gw, F1, FR, Mb on all maps) and the ultramafic Great Dyke are characterised by residuals with amplitudes of 35–55 mGal. Apparent anomaly closures and kinks along the linear, relatively narrow Great Dyke and Buhwa belt are due to undersampling along strike and the gridding process on unevenly spaced data, as evidenced by a comparison of the mapped geology and station locations (Figs. 1–3). The gravity highs are surrounded by gravity lows of -5 to -30 mGal corresponding to the granitic rocks, with most contacts marked by steep gradients (e.g., 5 mGal/km for Mb; Fig. 3). The main exception is the transition from the narrow (~ 5 km width) Buhwa belt (B) to the Limpopo (NMZ) granulite rocks which is associated with a very gentle gradient such that the contact between the two units is not discernible. In general, the

maxima of the gravity anomalies are interpreted to coincide with the axes of the belts and/or plutons, where the units probably attain considerable thickness.

There is no indication of gently dipping outward subsurface contacts as there is little or no continuation of anomalies beyond surface exposures; a rapid change in colour or a close contour spacing represents a steeper gravity gradient, which suggests a sub-vertical contact. Zones of steep gradients mark the granite-greenstone boundaries remarkably well (Figs. 3 and 5), except for the Fort Rixon (FR) belt. This has the smallest of the greenstone belt Bouguer gravity anomalies (~ 30 mGal) probably because it is the shallowest, with no southern closure of the -120 mGal contour that outlines the belt elsewhere. The anomaly also does not correlate well with the mapped geology, particularly in the east and northeast, possibly due to shallow dip-

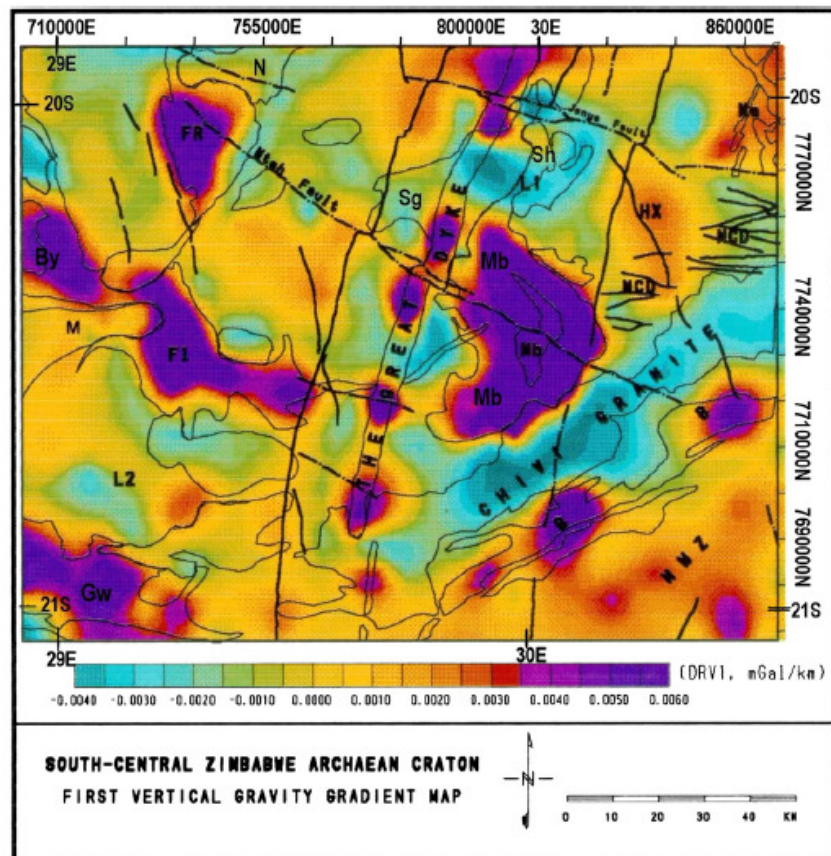


Fig. 6. First vertical gravity gradient map showing improved definition of geological boundaries (e.g., Mberengwa greenstone belt, Mb). Labels for geological units as in Figs. 1 and 2, and gravity anomalies L1, L2 and HX are discussed in text.

ping contact with low density pluton in the area (Figs. 5 and 6). The gravity data suggest a much smaller body, with the anomaly appreciably shifted both to the south and west. According to Harrison (1969), it can be imagined that successive periods of intrusion and granitisation have encroached upon the belt, causing a progressive decrease in its size. A large gravity low is observed east of the belt, encompassing a number of isolated granite outcrops and suggesting that they represent cupolas of a larger granitic mass at depth.

There is a marked correspondence between the NE-trending Chivi granite batholith and the lowest (up to -30 mGal) residual gravity values. This elongated granite pluton has a linear extent of nearly 150 km and a width ranging from 15 to 30 km (Fig. 1). Another relatively large EW- to NE-trending low (anomaly L1 on Figs. 5 and 6) under the north end of the Belingwe belt is also associated

with a pluton (Sg) whose effects swamp the 'snake head'-shaped part of the belt (Sh, Figs. 1 and 5) and a section of the Great Dyke in that area. This is interpreted to reflect large areal and depth extents for the pluton, although the anomaly could be constrained by better gravity station coverage, particularly on its western end. An interesting NE-trending small amplitude gravity high (HX) is observed northeast of the Belingwe belt over the Mashava tonalite and terminates against the Jenya fault. Proximity to Mashava (Ma) and Zvishavane ultramafic bodies points to a probable ultramafic composition/origin for the anomaly source and this is discussed further below (part (c)). Another important observation is that the small greenstone remnants north of Gwanda (Gw) have an appreciable high, which implies these are more extensive than their surface exposures. Adjacent to this are two lows, one associated

with a mapped pluton, the other corresponding to anomaly L2 (Fig. 5) possibly due to a concealed pluton.

The most surprising thing is that there is not a Bouguer gravity anomaly associated with the porphyritic Mbalabala pluton (M, Figs. 1 and 5) intruding west of Filabusi and almost cutting the latter off from the Bulawayo belt (By). This suggests that it has no, or a small, density contrast with the surrounding tonalites and gneisses, both at the surface and also subsurface. Alternatively, there could be greater variation in the composition of this granite with depth. Based on the measured densities (Table 1), the pluton is probably of the syn-volcanic, tonalitic Sesombi type rather than the post-tectonic Chilimanzi type characterized by gravity lows (e.g., Chivi and Nalatale granites, Figs. 1, 3, 5).

The Bouguer gravity map suggests that long wavelength anomalies are absent or minimal within the craton area, except over part of the Limpopo belt. Based on gravity and seismic reflection data, the Zimbabwe craton is about 35 km thick while the Limpopo belt in southern Zimbabwe ranges from 34 km (NMZ) to 29 km (CZ) (Stuart and Zengeni, 1987; Gwavava et al., 1992). The broad gravity high in the southeast of the map over the NMZ granulites is thus likely to be due to crustal thinning, as these rocks have relatively similar densities to cratonic granitoids (Gwavava, 1990; Gwavava et al., 1992). The alternative interpretation by Rollinson and Blenkinsop (1995), that the regional anomaly could be due to dense ultramafic and greenstone inclusions within the granulites, is questionable. Rollinson and Blenkinsop (1995) stress that the dominant NMZ lithologies are plutonic igneous rocks, and that supracrustal rocks are comparatively rare. Further, these inclusions form narrow layers (~100 m; op. cit) and therefore cannot account for the regional nature of the gravity high. Processed magnetic data confirm the linear form of the inclusions and Euler inverse models indicate that source bodies lie at depths less than about 2 km (Ranganai, 1995), implying small contributions to the gravity effect, if any. The Bouguer gravity high is also suppressed by the second vertical derivative process (Ranganai, 1995) which enhances local anomalies, confirming the regional nature of the anomaly. That is, the anomaly is not due to local features.

6.2. Vertical gravity gradient map

In order to improve the definition of geological boundaries, a first vertical derivative map of the gravity field was prepared (Fig. 6). The improvement is possible because the rate of change of gravity with elevation is much more sensitive to changes in rock densities occurring near the ground surface than to changes occurring at depth (Gupta and Grant, 1985). The effect is to sharpen anomalies caused by abrupt lateral changes in near-surface densities at the expense of broader anomalies caused by deeper or more gradual density changes (Simpson et al., 1986). The increased resolution stems from the lack of, or minimal,

anomaly overlapping effects. This is particularly evident on the western part of the Filabusi belt (FI) where a “break” between this belt and the Bulawayo greenstone belt to the west is now evident (see discussion in part (c) below). The Mbalabala pluton (M, Figs. 5 and 6) and its margin with the Filabusi belt is now well mapped, the latter now clearly separated from the Bulawayo belt (By).

In the granitic area between the Gwanda and Filabusi belts, the anomalies due to the known pluton south of the latter and its inferred subsurface southern satellite (L2) have been separated. In the northeast corner of the study area, isolation of anomaly HX northeast of the Belingwe belt is obvious, and there is a coincidence of the Jenya fault and vertical gradient contour breaks. As well as edge detection, the process of first vertical derivation also leaves some intermediate wavelengths and can therefore be used to map sub-cropping sources. Fig. 7 presents plots of first and second vertical derivative along a profile (XX', Figs. 2 and 3) across the Belingwe belt and Great Dyke to emphasize contact mapping. A striking feature of the profiles is that they are very similar in form and the zero values of both derivatives occur along the edges of the bodies. The first vertical derivative only displays such features for steeply dipping boundaries (e.g., Rudman et al., 1971; Thurston and Brown, 1994), and therefore, we infer the existence of such contacts from these data (e.g., for the Great Dyke, GD). Note also the coincident highs in the eastern end of the profiles due to the interpreted ultramafic sill discussed in part (a) above (anomaly HX, on Figs. 5 and 6).

In the southeast, there is also now a subtle indication of the Buhwa belt-NMZ (i.e. Craton-Limpopo Belt) boundary which was absent in the Bouguer gravity anomaly and residual gravity maps. Results of a detailed (1 km spacing) traverse across the belt and the mapped contact (Ranganai, 1995) indicate that gravity mapping of the contact is possible. Elsewhere, inadequate gravity data coverage precludes mapping of the contact. However, the aeromagnetic anomalies clearly define the boundary between the craton and the Limpopo belt (NMZ), the latter marked by large positive values (Ranganai et al., 1994). Similar magnetic signatures have been observed at the South Marginal Zone-Kaapvaal craton boundary (de Beer and Stettler, 1992).

6.3. Mapping hidden plutons, greenstone remnants and other units/features

Significant new observations from the combination of maps presented include a gravity high (HX, Figs. 3, 5 and 6) northeast of the Belingwe greenstone belt, and southwest of the Mashava Ultramafic Complex (Ma). This gravity anomaly has an associated, approximately rectangular, magnetic high that is bounded by the East and Sebang Poort dykes, the Jenya fault and the Chivi granite (Fig. 8). Thus, the highs could be due to a high density, high magnetization ultramafic body concealed within the

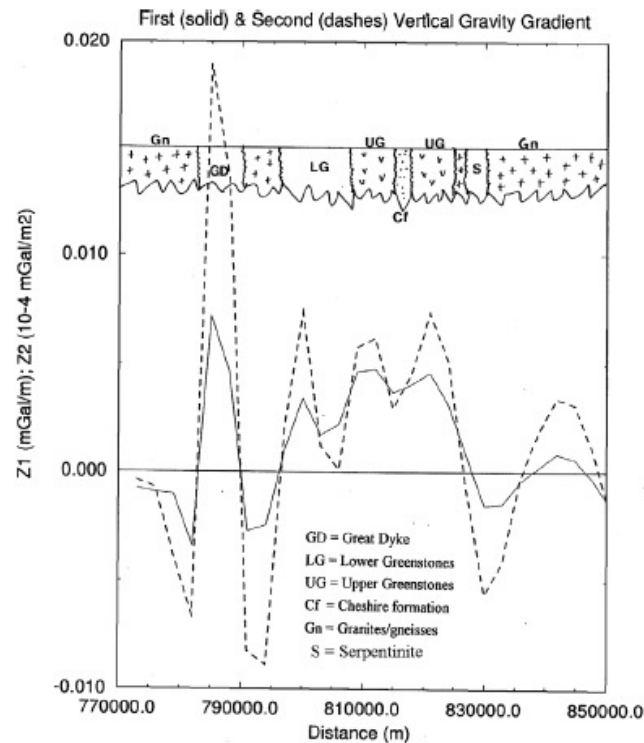


Fig. 7. First (solid) and second (dashes) vertical gravity gradient profiles across the Great Dyke and the Mberengwa greenstone belt. Note that both derivatives have their zero values approximately at the contacts of different units, implying steeply dipping geological units.

tonalitic granites (Table 1). This interpretation is supported by the identification of a buried southerly extension of the Mashava complex (Fig. 8; Ranganai, 1995) and the proximity of other such intrusions west and southwest of this new body (e.g., Zvishavane, Figs. 1 and 8). Although the gravity anomaly amplitude is only ~ 10 mGals, it is probable that the remnants are too small to show up clearly on the gravity maps, but can still produce a large magnetic high. Fig. 8 also shows several other new features and structures, such as a northern member (Zn) of the Zvishavane ultramafic complex (Z), and faults (F1 and F2) on the edges of anomaly HX (Fig. 8).

One of the features discovered in this study is a deep ENE-WSW-trending structure cutting across the north-central part of the study area, evident particularly in the Bouguer gravity contour map (gentle gradient labelled W–E on Fig. 3). The evidence for this apparently deep-seated crustal structure on the geological map is the break between the Filabusi and Fort Rixon belts, the pinching of the Belingwe belt, and the Jenya fault marking the southern edge of the Mashava Ultramafic Complex (Ma) in the northeast of the area. This is supported by aeromagnetic

data that also indicate a NE/SW-striking ~ 3 km wide shear zone on the northwestern and southeastern edges of the Filabusi and Fort Rixon greenstone belts, respectively (Ranganai et al., 1994; Ranganai, 1995). The latter coincides with the “break” between the Bulawayo and Filabusi greenstone belts discussed on the vertical gravity gradient map above (Fig. 6). The significance of this structure is not yet clear but it is in places coincident with pluton edges (Shabani granite, Sg, Figs. 1, 5 and 6) and a fault.

7. Modelling and interpretation

7.1. Gravity expression of the granite-greenstone field relationship

The Bouguer gravity anomaly map and its derivatives provide a comprehensive view of the areal extent of the major geological units and reflect the gross, crustal structure of the area. Pronounced gravity highs and steep gradients correspond with the mapped margins of all the greenstone belts, with little or no lateral continuation of units under cover beyond mapped exposures. The positive

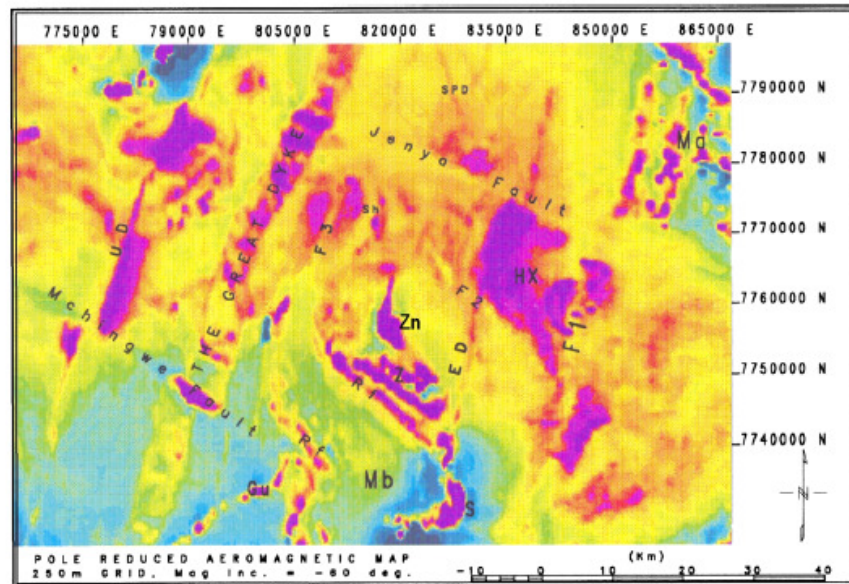


Fig. 8. Reduced to the pole (RTP) aeromagnetic data of the northern part of the Mberengwa (Belingwe) greenstone belt. Note the magnetic highs over the Great Dyke and its satellites (UD and ED), and over ultramafic intrusions (e.g., Ma, Z, Zn, S and Gu), where they map these features very well (cf. Fig. 1). Anomaly HX with corresponding Bouguer gravity high interpreted as another ultramafic body as discussed in text.

and negative anomaly axes coincide with the inferred synformal and antiformal greenstones and granites, respectively (cf. Subrahmanyam and Verma, 1982), typical of many Archaean granite-greenstone terrains (e.g., Gupta et al., 1982; Gupta and Grant, 1985). The steep gradients indicate steeply dipping contacts for the anomalous bodies that, in turn, suggest an intrusive relationship between the granites and greenstones, a hypothesis which we test below. The greenstone belts appear to be considerably deformed and altered by the younger, intrusive granitic plutons (cf. Drury, 1977; Gorman et al., 1978; Minnitt and Anhaeusser, 1992; Bouhallier et al., 1993). The anomaly shapes of these plutons are consistent with their emplacement as either elongate batholiths and/or circular stocks (cf. Szewczyk and West, 1976).

The general NE/SW to EW trend of gravity lows associated with the (2.6 Ga) Chilimanzi suite plutons (e.g., Chivi granite, Sg-L1, L2; Figs. 5 and 6) probably indicates a direction of weakness in the crust around the time of the intrusion. This is thought to be due to effects of the Limpopo Belt-related deformation (NW-directed thrusting onto the craton), particularly in the vicinity of the Limpopo Belt margin (Robertson, 1973, 1974; Coward et al., 1976; Mkweli et al., 1995; Frei et al., 1999). The influence of the NW-directed thrusting dies out northwards, where the plutons take an EW trend rather than the NE direction of the NMZ. Post-deformation that elongated plutons along this trend is considered unlikely as they are generally unde-

formed except at their margins (Frei et al., 1999). Treloar and Blenkinsop (1995) suggest that the Chilimanzi suite may be localized along a system of large intracontinental conjugate ESE-dextral and NNE-sinistral shears in the craton. The ~NE/SW trend of the plutons is one of five regional lineament directions apparent on the magnetic anomaly maps, corresponding to dykes, faults and other geological units, e.g., Great Dyke (Ranganai et al., 1994; Ranganai, 1995).

The regional gravity field shows no evidence for significant crustal thickness variations in most of the area (cf. Fig. 3), and seismic studies indicate that the crust under the Zimbabwe craton is about 35 km thick (Stuart and Zengeni, 1987; de Beer and Stettler, 1992). This is supported by the small range of -105 to -115 mGal for the simple 'isostatic' regional (Simpson et al., 1986; A.B. Reid, pers. comm. 1995) computed by upward continuing the Bouguer gravity grid to 35 km as discussed earlier. Density measurements (Table 1 and Fig. 4) together with the apparent density map (Fig. 9) suggest that the observed anomalies can be explained by upper crustal lateral density variations alone, rather than changes in thickness of prisms and mode of compensation (cf. Simpson et al., 1986). Values from the latter are comparable to the laboratory determinations from hand specimen for granites but are rather lower than the measured volcanic densities. The only exception to this interpretation is the general gravity high over the NMZ granulites which is attributed to crustal

thinning, as these rocks have similar densities to cratonic granitoids (Gwavava et al., 1992). Gwavava et al. (1996) also computed an isostatic gravity anomaly map of the Limpopo belt and parts of the adjacent cratons that is characterised by a positive anomaly over the SMZ and a negative anomaly over the NMZ. These differences are explained as due to the presence of dense granulites within the upper crust in the SMZ and due to recent rapid erosion in the NMZ.

7.2. Granite-greenstone subsurface relationship

To test the existence of steep subsurface contacts implied by gravity data, 2^{1/2}D modelling (e.g., Won and Bevis, 1987) of two profiles across the Belingwe and Fort Rixon greenstone belts has been carried out (see Figs. 2 and 3

for profile location). The two greenstone belts have been selected because they produce the largest (~60 mGal) and smallest (~30 mGal) gravity anomalies, respectively. The data points were extracted from the main raw data set (original station values) by projecting points within a 3 km swath width onto a profile. As granites completely surround the greenstone belt, a simplifying assumption that it is everywhere floored by granite has been made. We here define our basement as the granites older than 2.7 Ga, the age of the dominant Upper Greenstones: the ~2.9 Ga gneisses/tonalites and older gneisses that are known to form the basement to both the Lower and Upper greenstones (e.g., Bickle et al., 1975, 1994). All greenstone belts under consideration are of at least this age, and this classification is in line with density measurements (Table 1 and Fig. 4). In addition, the dominant Upper Greenstone

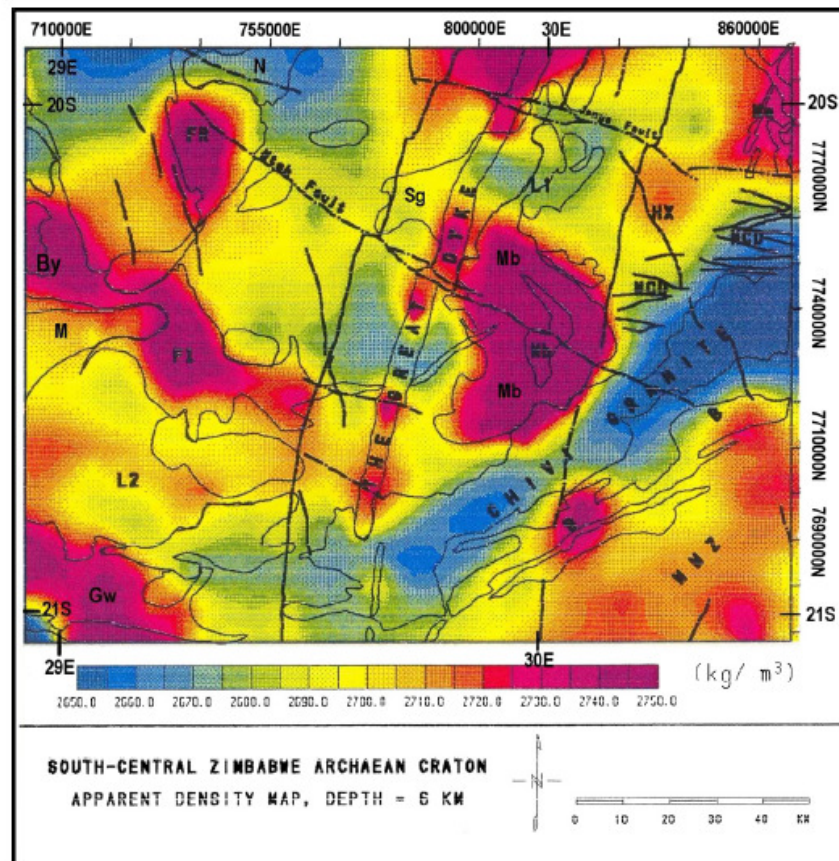


Fig. 9. Apparent density map showing a reasonably good correlation between the apparent densities and the mapped geology (e.g., Chivi granite and Mberengwa greenstone belt). Inversion with a 'prism/plate' thickness of 6 km based on gravity derived depth extent of the Mberengwa greenstone belt (Ranganai, 1985).

basalts are quite homogeneous and therefore the greenstone belts can be modelled with uniform density. The modelling was carried out using the mean of the measured densities (Table 1 and Fig. 4), plus the known surface geology as constraints. Profile XX' includes the Great Dyke and densities here are based on values from Podmore (1985), and Podmore and Wilson (1987). No attempt was made to reproduce every detail of the observed anomalies and the models are probably the simplest that broadly satisfy the surface geology, the density measurements and the gravity field. Conclusions regarding the broad-scale structure of the belts are not significantly affected by these limitations/assumptions.

We modify the geological models of Nisbet et al. (1993) with interpretations of regional gravity data constrained by rock density and other geological and geophysical data (Figs. 10 and 11). A comparison of model and observed anomalies shows that the broad positives are caused by moderately steep-sided volcanic bodies within the granitic crust. They do not support a wide, deep root for the bodies, but narrow feeders of considerable depth extent could also be present. A range of models were produced for each greenstone belt (Ranganai, 1995) and, in general, all have similar geometries. Differences in density contrast change the thickness of the various bodies by approximately ± 200 m (or $\sim 10\%$), but this does not affect the overall structural concept of the cross-sections. They are considered to be the most likely interpretation of the subsurface geometry of the units because they satisfy different constraints. The Belingwe belt model (Fig. 10) has a 5.0 ± 0.2 km thick basin-shaped pile of volcanics, capped by a thin layer (~ 400 m) of sediments at the centre. Note that the granite contact in the east is the known unconformity (Bickle et al., 1975, 1994) and is therefore not an

intrusive contact as in the west. For both contacts, the steep dips near the surface in our models are constrained by field observations (dip $> 70^\circ$; Martin, 1978). Models of thrust geometries cannot reproduce the sharp gradients at the edges of the bodies. Further, the aeromagnetic data from the region (e.g., Fig. 8; Ranganai, 1995) do not show any evidence of thrust tectonics that would be associated with tectonic emplacement of crustal fragments (the "Mberengwa Allochthon" of Kusky and Kidd, 1992).

For the Fort Rixon greenstone belt, the modelled profile is located towards the southern edge of the belt (Figs. 1 and 2). However, due to the asymmetry of the Bouguer gravity anomaly towards the southwest mentioned earlier, the profile covers the peak anomaly, and hence the thickest part of the belt. The resulting gravity model (Fig. 11) indicates that the thickness of the belt is limited to the range: 3–4 km. The western contact is particularly domal in shape, consistent with an intrusive relationship. It is thought that a large intrusive granite (Fig. 1) separates this belt from the main Bulawayo/Filabusi greenstone belt (Wilson, 1981, 1990). This suite of late plutons has similar densities to the older 'basement' gneisses and tonalites (Ranganai, 1995), and therefore we do not observe any Bouguer gravity low over the suspected pluton. In order to obtain a good fit between the observed and calculated Bouguer gravity values, a thin layer of the volcanics has been extended westward beyond the mapped exposure. Based on aeromagnetic data and field mapping (Ranganai, 1995; Wilson, 1990) the steeper eastern flank is considered to be a shear or detachment zone along which the Bulawayo/Filabusi-Fort Rixon belt separation was effected. The Irisvale-Lancaster shear zone (ILSZ, Fig. 1) runs along the ESE margin of the belt, striking NNE to SSE and continuing to the SSW, to the Filabusi greenstone belt and beyond. Note that in the model

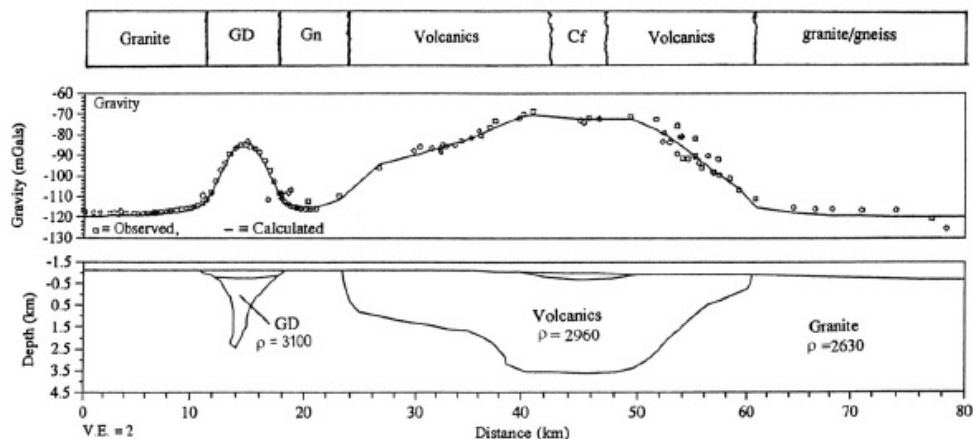


Fig. 10. Mberengwa Greenstone Belt and Great Dyke $2\frac{1}{2}$ D models for profile XX' (see Figs. 2 and 3 for location). VE = vertical exaggeration (2), Gn = granite/gneiss, GD = Great Dyke, Cf = Chesire formation sediments. Densities (ρ) in kg/m^3 . VE = vertical exaggeration (2). The surface of the model relates to the topography.

Please cite this article in press as: Ranganai, R.T. et al., Gravity anomaly patterns in the south-central Zimbabwe ..., J. Afr. Earth Sci. (2008), doi:10.1016/j.jafrearsci.2008.01.011

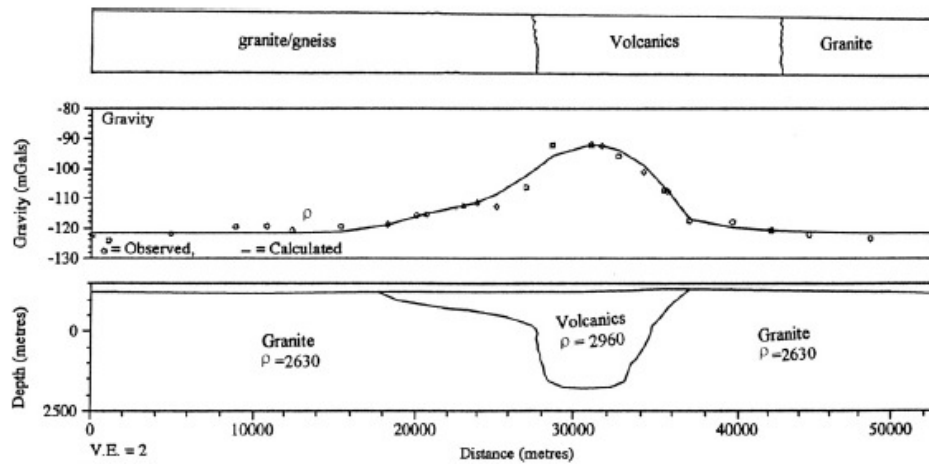


Fig. 11. Fort Rixon Greenstone Belt $2\frac{1}{2}$ D Model for profile YY' (see Figs. 2 and 3 for location). Densities (ρ) in kg/m^3 . VE = vertical exaggeration (2). The surface of the model relates to the topography.

the greenstone margin occurs almost 4 km west of the contact on the geological cross-section. This configuration is clearly a result of the intrusion and granitisation of the belt by the intrusive Nalatale granite that outcrops to the northeast of the profile (Figs. 1 and 2). It is highly probable that this granite underlies much of the eastern parts of the Fort Rixon greenstone belt.

All the greenstone belts under investigation have comparable anomaly amplitudes and measured densities and thus it is plausible to infer that they also have similar depth extents. These are relatively smaller than the mapped stratigraphic thicknesses of up to 9.5 km, which may be overestimated due to tectonic repetition or stacking (Martin, 1978; Gorman et al., 1978; Gupta et al., 1982; Jelsma and Dirks, 2000). The gravity data show that the greenstone belts are not deep synclinal keels. The modelled thicknesses are consistent with results from spectral analysis of the Bouguer gravity data revealing density discontinuities at 3.0, 5.0 and 9–10 km depths, and 3D Euler deconvolution with significant solutions showing a 3.0–5.0 km depth range (Ranganai, 1995). We can compare our results with greenstones on other cratons where more accurate deep crustal information is available from deep seismic reflection data and/or geoelectrical soundings, such as from Australia, Canada and South Africa (e.g., Green et al., 1990; Goleby et al., 1994; Stettler et al., 1997). The seismic and electrical results also show that the Archaean greenstone belts have a predominantly flat base, implying a simple structural relationship between the greenstones and the underlying granites (Drummond et al., 1993; Goleby et al., 1994; Stettler et al., 1997). Aspect ratios of nine well-known greenstone belts from five different cratons range from 4 to 38 (De Wit and Ashwal, 1997b). However, despite these strong similarities, a single tectonic

environment applicable to all greenstone belts does not exist.

Prior to these studies, a continental rift environment had been proposed for the Upper Greenstones, and to some extent, the Lower Greenstones (Wilson et al., 1978; Nisbet et al., 1981; Bickle and Nisbet, 1993; Campbell et al., 1992; Jelsma et al., 1996; Blenkinsop et al., 1997). Both the qualitative and forward modelling results support the hypothesis that development of the greenstone belts involved deposition of volcanics in (intracontinental) rift zones (Wilson et al., 1978; Barton and Key, 1981; Compston et al., 1986) or fault-bounded basins (cf. Gorman et al., 1978; Barton and Key, 1981). These were laid on older granitic crust (Bickle et al., 1975, 1994; Nisbet, 1987; Bickle and Nisbet, 1993; Blenkinsop et al., 1993, 1997) and subsequently deformed during intrusion of granitic plutons (cf. Drury, 1977; Schwerdtner et al., 1979; Mareschal and West, 1980; Gupta et al., 1982; Minnitt and Anhaeusser, 1992; Bouhallier et al., 1993; Jelsma et al., 1993, 1996). Seismic and geochronological data from the Abitibi granite-greenstone terrain show that extensional structures were largely overprinted by the effects of later compressional movements (Green et al., 1990), providing evidence for greenstone deformation by pluton emplacement. Coincidence of Bouguer gravity anomaly axes with thickest parts of greenstones and plutons, steep dips and gravity gradients, and absence of evidence for thrust tectonics, and other evidence are all inconsistent with an allochthonous origin.

8. Discussion

A rifting history for the greenstone belts is partly supported by gravity models of the Great Dyke (Fig. 10; and

Podmore and Wilson, 1987) which show either a V-shaped or a Y-shaped cross-section, the latter comprising a dyke-like feeder. It is worth noting that the Great Dyke has been interpreted by some workers as a failed rift and/or an abortive greenstone belt (Coward et al., 1976; Wilson et al., 1978). In the greenstone belts, the 'dyke root' was probably destroyed during subsequent tectono-magmatic activity (e.g., magmatic stoping, Gorman et al., 1978; Gupta et al., 1982), most probably associated with voluminous, crustally derived late (2.6 Ga) Sesombi and Chilimanzu suite plutons. As no major plutonic activity occurred in the 'stable craton' after the Great Dyke intrusion at 2.5 Ga (Wilson, 1979, 1981, 1990; Taylor et al., 1991; Frei et al., 1999), its 'feeder dyke' may be 'preserved'.

Accepting an ensialic origin for the greenstone belts, we propose a schematic model for the late Archaean to early Proterozoic tectonic environment below. In proposing the synoptic scenario, it should be kept in mind that geophys-

ical data alone cannot retrace the scheme of Archaean tectonics but offer tests of and constraints on geological and geochemical models. Fig. 12 is a schematic representation of these events based on the geological models discussed above and the new geophysical constraints offered by this study. During stage 1 (ca. 2.9 Ga), the rift zones are envisaged to have developed in response to the rise of mantle diapirs/plumes, and regional crustal extension and thinning (e.g., McKenzie et al., 1980; Bickle and Eriksson, 1982; Middleton, 1984; Ayres and Thurston, 1985; Nisbet et al., 1981, 1993; Jelsma et al., 1996). Rifting resulted in volcanism, loading the thin crust with dense volcanics, subsidence and sedimentation (stages 2 and 3; ~2.7 Ga). The small proportion of resedimented volcanics in many of the greenstone belts of the craton (Wilson, 1979, 1981) implies rapid basin subsidence during the volcanic phase (Nisbet et al., 1993). Furthermore, unlike uplift above subduction zones, crustal extension only causes localized uplift

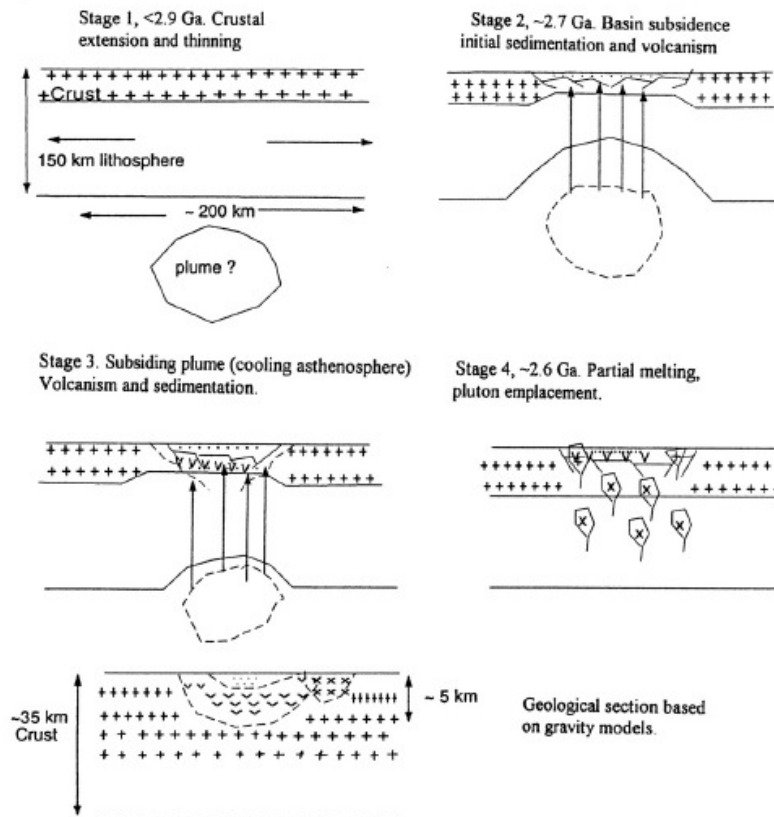


Fig. 12. Proposed development of greenstone belts of the study area from the late Archaean, based on rift models and the gravity models (Figs. 10 and 11) as discussed in text. Symbols: + = gneissic basement; v = volcanics; x = post-volcanic plutons, and = = sediments.

of fault blocks followed by subsidence, ensuring that any sediments produced during the rifting phase are deposited rapidly and not reworked (Hunter et al., 1998). Sm-Nd model ages from the Ngezi Group (Upper Greenstones) in the Belingwe belt relate to the basement terrain and REE patterns and Sm-Nd ratios confirm the localized sediment derivation (Bickle and Nisbet, 1993; Hunter et al., 1998). A simple interpretation of the correlation of the Ngezi Group across the craton (Wilson et al., 1978, 1995; Taylor et al., 1991) is that the greenstone belts are separate, individual rifts that formed simultaneously (Nisbet et al., 1981; Hunter et al., 1998). At the end of stage 3, the lithosphere finally re-establishes its original thickness as the asthenosphere cools.

In stage 4 (2.6–2.7 Ga), partial melting in the lower crust (and upper mantle) created a convecting tonalitic magma layer (cf. Ridley and Kramers, 1990), leading to pluton emplacement. At the same time, deformation of the volcano-sedimentary sequences is caused by both vertical and horizontal forces, as demonstrated by the gravity and aeromagnetic data, respectively (cf. Wilson, 1990; Jelsma et al., 1993, 1996; Ranganai, 1995; Treloar and Blenkinsop, 1995). The former is predominantly at the local scale due to pluton emplacement (Wilson, 1979; Jelsma and Dirks, 2000) while the latter is of regional scale, involving movements between the Zimbabwe craton and the Limpopo Belt (Wilson, 1990; Treloar and Blenkinsop, 1995; Dirks and Jelsma, 1998). Ages of the widespread plutons marginal to the greenstone belts range from 2.63 to 2.58 (e.g., Hickman, 1978; Taylor et al., 1991; Mkweli et al., 1995; Frei et al., 1999), while the Limpopo orogeny took place between 2.70 and 2.65 Ga (e.g., van Reenen et al., 1992; Treloar and Blenkinsop, 1995). In early Proterozoic times (2.5–2.0 Ga), continued movements involving the Zimbabwe craton and the Limpopo Belt led to the emplacement of the Great Dyke, and development of structures cutting across greenstones.

9. Conclusions

A new detailed Bouguer gravity map of the southern Zimbabwe craton and northern Limpopo orogenic belt region has been constructed, shedding light on the geological evolution of this important region. The high density of the greenstones and the low density of the granite plutons are reflected in their spatial correlation with local positive and negative Bouguer gravity anomalies, respectively. Several conclusions can be drawn from the study. Firstly, the well-defined anomalies and their derivatives have allowed the mapped geology to be extrapolated and boundaries positioned confidently. Several important features, not clearly identified by geologic mapping alone, are recognised; these include plutons, greenstone remnants and other structural features. Locally, positive Bouguer gravity anomalies correlate with basic/ultrabasic intrusions interpreted from aeromagnetic data and satellite imagery.

Secondly, in general, the regional gravity field shows no evidence of crustal thickness variation and anomalies can be explained by density variations within the upper 10 km of the crust. Although regional effects cannot be ruled out, there is no direct evidence for their existence in most of the study area, the exception being the southeastern corner (Limpopo belt boundary) where gravity highs have been shown to be due to crustal thinning (Gwavava et al., 1992).

The third point to note is that alternating gravity highs and lows map inferred synforms (sinks of Gorman et al., 1978) and antiforms filled with high density volcanics and low density granitic cores, respectively. This pattern also suggests that the greenstone depositories were not much larger than their present mapped areas, and the current positions approximate to their original locations (Nisbet et al., 1981; Ranganai, 1995; Campbell et al., 1992; Bickle and Nisbet, 1993). The circular and elongate sub-oval gravity lows corresponding to known and concealed plutons confirm the two main modes of their emplacement: stocks and 'deep-rooted' batholiths (Szewczyk and West, 1976; Subrahmanyam and Verma, 1982). For both greenstone belts and plutons, there is a marked correspondence of margins with steep gravity anomaly gradients.

A 2.5 dimensional modelling indicates the thickness of the Belingwe and Fort Rixon greenstone belts to be ~5 and ~3 km, respectively. Granite-greenstone contacts are shown to be sub-vertical and/or domal, consistent with either an unconformable or an intrusive relationship. Although the models do not rule out an allochthonous relation, the preceding observation on greenstone location plus other structural and geochemical considerations (e.g., Blenkinsop et al., 1993, 1997; Hunter et al., 1998) make this highly improbable.

Finally, as a result of the present studies and previous geological and geophysical work, a hypothesis for the evolution of the greenstone belts can be suggested: eruption of volcanics through older sialic basement and deposition in fault-bounded rift basins (Wilson et al., 1978; Barton and Key, 1981; Gupta et al., 1982; Bickle and Nisbet, 1993), followed by deformation and erosion. Intruding granitic plutons imparted steep dips to the volcanics and granitised them (Gorman et al., 1978; Minnitt and Anhaeusser, 1992; Bouhallier et al., 1993; Jelsma et al., 1993, 1996), resulting in the basin-like structures of limited depth extent. This is followed by late-stage strike-slip activity, producing cross-cutting structures some of which were intruded by mafic dykes.

Acknowledgements

The Commonwealth Scholarship Commission, the British Council, University of Zimbabwe Physics Department, the Zimbabwe Geological Survey and the Zimbabwe Republic Police provided financial and logistical support for the gravity survey. We thank NERC Geophysical Equipment Facility for use of GPS receivers. The help,

general assistance and co-operation of D.L. Jones before and during the fieldwork is acknowledged. Thanks to the field crew, and to Mike Hapanyengwi and Oswald Gwavava who assisted with the density measurements. The paper benefited from a critical review by Alan Reid and Tom Blenkinsop. We thank the reviewers for their constructive comments.

References

- Ayres, L.D., Thurston, P.C., 1985. Archean supracrustal sequences in the Canadian Shield: an overview. In: Ayres, L.D., et al. (Eds.), *Evolution of Archean Supracrustal Sequences*. Geological Association Canada Special Paper 28, pp. 343–380.
- Barton, J.M., Key, R.M., 1981. The tectonic development of the Limpopo mobile belt and the evolution of the archaean cratons of southern Africa. In: Kroner, A. (Ed.), *Precambrian Plate Tectonics*. Elsevier, Amsterdam, pp. 185–212.
- Bickle, M.J., Eriksson, K.A., 1982. Evolution and subsidence of early Precambrian sedimentary basins. *Philosophical Transactions Royal Society London A305*, 225–247.
- Bickle, M.J., Martin, A., Nisbet, E.G., 1975. Basaltic and peridotitic komatiites and stromatolites above a basal unconformity in the Belingwe greenstone belt, Rhodesia. *Earth Planetary Science Letters* 27, 133–139.
- Bickle, M.J., Nisbet, E.G. (Eds.), 1993. *The geology of the Belingwe greenstone belt, Zimbabwe: a study of the evolution of Archean continental crust*. Geol. Soc. Zimbabwe Special Publ. 2, A.A. Balkema, Rotterdam, p. 239.
- Bickle, M.J., Nisbet, E.G., Martin, A., 1994. Archean greenstone belts are not oceanic crust. *The Journal of Geology* 102, 121–138.
- Blakely, R.J., 1995. *Potential Theory in Gravity and Magnetic Applications*. Cambridge University Press, p. 441.
- Blenkinsop, T.G., Fedo, C.M., Bickle, M.J., Eriksson, K.A., Martin, A., Nisbet, E.G., Wilson, J.F., 1993. Ensilic origin for the Ngezi group, Belingwe greenstone belt, Zimbabwe. *Geology* 21, 1135–1138.
- Blenkinsop, T.G., Martin, A., Jelsma, H.A., Vinyu, M.L., 1997. The Zimbabwe craton. In: de Wit, M.J., Ashwal, L.D. (Eds.), *Greenstone Belts*, Oxford Monograph on Geology and Geophysics. Clarendon Press, Oxford, pp. 567–580.
- Bouhallier, H., Choukroune, P., Balkev, M., 1993. Diapirism, bulk homogeneous shortening and transcurrent shearing in the Archean Dharwar craton, the Holenarsipur area, southern India. *Precambrian Research* 63, 43–58.
- Campbell, S.D.G., Oesterlen, P.M., Blenkinsop, T.G., Pitfield, P.E.J., Munyanyiwa, H., 1992. A Provisional 1:2 500,000 scale Tectonic map and the tectonic evolution of Zimbabwe. *Annals of the Zimbabwe Geological Survey XVI* (1991), 31–50.
- Campbell, S.D.G., Pitfield, P.E.J., 1994. Structural controls of gold mineralization and regional structure in the Mberengwa greenstone belt. Midlands Goldfield Project-Zimbabwe, Phase II (1992–1994) Final Report No. 12, Harare, p. 24.
- Card, K.D., 1990. A review of the superior province of the Canadian shield, a product of Archean accretion. *Precambrian Research* 48, 99–156.
- Compston, W., Williams, I.S., Campbell, I.H., Gresham, J.J., 1986. Zircon xenocrysts from the Kambalda volcanics, age constraints and direct evidence for older continental crust below the Kambalda-Norseman greenstones. *Earth Planetary Science Letters* 76, 299–311.
- Condie, K.C., 1981. Archean greenstone belts. *Developments in Precambrian Geology*, vol. 1. Elsevier, Amsterdam.
- Coward, M.P., James, P.R., Wright, L., 1976. Northern margin of the Limpopo mobile belt, southern Africa. *Geological Society America Bulletin* 87, 601–611.
- de Beer, J.H., Stettler, E.H., 1992. The deep structure of the Limpopo Belt from geophysical studies. *Precambrian Research* 55, 173–186.
- Wit, M.J., Roering, C., Hart, R.J., Armstrong, R.A., de Ronde, C.E.J., Green, R.W.E., Tredoux, M., Peberdy, E., Hart, R.A., 1992. Formation of an Archean continent. *Nature* 357, 553–562.
- De Wit, M.J., Ashwal, L.D. (Eds.), 1997a. *Greenstone belts*. Oxford Monograph on Geology and Geophysics. Clarendon Press, Oxford, p. 809.
- De Wit, M.J., Ashwal, L.D., 1997b. Preface: convergence towards divergent models of greenstone belts. In: De Wit, M.J., Ashwal, L.D. (Eds.), *Greenstone Belts*, Oxford monograph on geology and geophysics. Clarendon Press, Oxford, pp. ix–xvii.
- Dirks, P.H.G.M., Jelsma, H.A., 1998. Horizontal accretion and stabilization of the Zimbabwe craton. *Geology* 26, 11–14.
- Drummond, B.J., Goleby, G.R., Swager, C.P., Williams, P.R., 1993. Constraints on Archean crustal composition and structure provided by deep seismic sounding in the Yilgarn Block. *Ore Geology Reviews* 8, 117–124.
- Drury, S.A., 1977. Structures induced by granitic diapirs in the Archean greenstone belt at Yellowknife, Canada: implications for Archean geotectonics. *Journal of Geology* 85, 345–358.
- Fairhead, J.D., Watts, A.B., Chevalier, P., El-Haddadeh, B., Green, C.M., Stuart, G.W., Whaler, K.A., Windle, I., 1988. *African Gravity Project Technical Report*. University of Leeds Industrial Services, Leeds.
- Fedo, C.M., Eriksson, K.A., Blenkinsop, T.G., 1995. Structural geology and assembly of the Archean Bulwa Greenstone Belt and surrounding granite-gneiss terrane with implications for the evolution of the Limpopo Belt. *Canadian Journal Earth Sciences* 32, 1977–1990.
- Fedo, C.M., Eriksson, K.A., 1996. Stratigraphic framework of the ~3.0 Ga Bulwa Greenstone Belt: a unique stable-shelf succession in the Zimbabwe Archean craton. *Precambrian Research* 77, 161–178.
- Fisk, K., Hawadi, M.T., 1996. *The National Gravity Dataset of Zimbabwe: Zimbabwe Geological Survey Bulletin No. 103*, Harare, p. 39.
- Frei, R., Schoenberg, R., Blenkinsop, T.G., 1999. Geochronology of the late Archean Razi and Chilimanzi suites of granites in Zimbabwe; implications for the late Archean tectonics of the Limpopo Belt and Zimbabwe craton. *South African Journal Geology* 102, 55–63.
- Goleby, G.R., Drummond, B.J., Korsch, R.J., Wilcox, J.B., O'Brien, G.W., Wake-Dyster, K.D., 1994. Review of recent results from continental deep seismic profiling in Australia. *Tectonophysics* 232, 1–12.
- Gorman, B.E., Pearce, T.H., Birkett, T.C., 1978. On the structure of Archean greenstone belts. *Precambrian Research* 6, 23–41.
- Green, A.G., Mikereit, B., Mayrand, L.J., Ludden, J.N., Hubert, C., Jackson, R.H., Sutcliffe, R.H., West, G.F., Verpaalst, P., Simard, A., 1990. Deep structure of an Archean greenstone terrain. *Nature* 344, 327–330.
- Gupta, V.K., Grant, F.S., 1985. Mineral-exploration aspects of gravity and aeromagnetic surveys in the Sudbury-Cobalt area, Ontario. In: Hinze, W.J. (Ed.), *The Utility of Regional Gravity and Magnetic Anomaly Maps*, Society of Exploration Geophysicists, pp. 392–412.
- Gupta, V.K., Ramani, N., 1980. Some aspects of regional-residual separation of gravity anomalies in a Precambrian terrain. *Geophysics* 45, 1412–1426.
- Gupta, V.K., Thurston, P.C., Dusanowsky, T.H., 1982. Constraints upon models of greenstone belt evolution by gravity modelling, Birch-Uchi greenstones belt, Northern Ontario. *Precambrian Research* 16, 233–255.
- Gwavava, O., 1990. A regional gravity study of the Limpopo Belt and mechanisms of isostatic compensation in the region. Unpublished DPhil Thesis. University of Zimbabwe, Harare, p. 281.
- Gwavava, O., Swain, C.J., Podmore, F., Fairhead, D.J., 1992. Evidence of crustal thinning beneath the Limpopo Belt and Lebombo monocline of southern Africa based upon regional gravity studies and implications for the reconstruction of Gondwana. *Tectonophysics* 212, 1–20.
- Gwavava, O., Swain, C.J., Podmore, F., 1996. Mechanisms of isostatic compensation of the Zimbabwe and Kaapvaal cratons, the Limpopo Belt and the Mozambique basin. *Geophysical Journal International* 127, 635–650.

- Harrison, N.M., 1969. The geology of the country around Fort Rixon and Shangani. Rhodesia Geological Survey Bulletin 61, Salisbury, p. 152.
- Henkel, H., 1976. Studies of density and magnetic susceptibilities of rocks from northern Sweden. *Pure and Applied Geophysics (Pageoph.)* 114, 235–249.
- Hickman, M.H., 1978. Isotopic evidence for crustal reworking in the Rhodesian Archaean craton, southern Africa. *Geology* 6, 214–216.
- Hunter, M.A., Bickle, M.J., Nisbet, E.G., Martin, A., Chapman, H.J., 1998. Continental extensional setting for the Archaean Belingwe greenstone belt, Zimbabwe. *Geology* 26, 883–886.
- Jelsma, H.A., van der Beek, P.A., Vinyu, M.L., 1993. Tectonic evolution of the Bindura-Shamva greenstone belt (northern Zimbabwe): progressive deformation around diapiric batholiths. *Journal Structural Geology* 15, 163–176.
- Jelsma, H.A., Vinyu, M.L., Valbracht, P.J., Davies, G.R., Wijbrans, J.R., Verdurmen, E.A.T., 1996. Constraints on Archaean crustal evolution of the Zimbabwe craton: a U–Pb zircon, Sm–Nd and Pb–Pb whole-rock isotope study. *Contributions Mineralogy Petrology* 124, 55–70.
- Jelsma, H.A., Dirks, P.H.G.M., 2000. Tectonic evolution of a greenstone sequence in northern Zimbabwe: sequential early stacking and pluton diapirism. *Tectonics* 19, 135–152.
- Kusky, T.M., Kidd, W.S.F., 1992. Remnants of an Archaean oceanic plateau, Belingwe greenstone belt, Zimbabwe. *Geology* 20, 43–46.
- Kusky, T.M., Winsky, P.A., 1995. Structural relationships along a greenstone/shallow water shelf contact, Belingwe greenstone belt, Zimbabwe. *Tectonics* 14, 448–471.
- Mareschal, J.C., West, G.F., 1980. A model for Archaean tectonism. Part 2. Numerical models for vertical tectonism in greenstone belts. *Canadian Journal Earth Sciences* 17, 60–71.
- Martin, A., 1978. The geology of the Belingwe-Shabani schist belt. Rhodesia Geological Survey Bulletin 83, Salisbury, p. 220.
- McKenzie, D.P., Nisbet, E.G., Sclater, J.G., 1980. Sedimentary basin development in the Archaean. *Earth Planetary Science Letters* 48, 35–41.
- Middleton, M.F., 1984. Formation of rifted continental margins: a discussion of mechanisms. *First Break*, April, pp. 9–14.
- Minnitt, R.C.A., Anhaeusser, C.R., 1992. Gravitational and diapiric structural history of the eastern portion of the Archaean Murchison greenstone belt, South Africa. *Journal African Earth Sciences* 15, 429–440.
- Mkweli, S., Kamber, B., Berger, M., 1995. Westward continuation of the craton-Limpopo Belt tectonic break in Zimbabwe and new age constraints on the timing of the thrusting. *Journal Geological Society London* 152, 77–83.
- Moniz, H., 1984. Geodetic Reference System 1980. *Bulletin of Geodesy* 58, 388–398.
- Myers, J.S., 1995. The generation and assembly of an Archaean super continent: evidence from the Yilgarn craton, western Australia. In: Coward, P., Ries, A.C. (Eds.), *Early Precambrian Processes*, vol. 95. Geological Society Special Publication, pp. 143–154.
- Nisbet, E.G., 1987. *The Young Earth: an Introduction to Archaean Geology*. Boston, Allen and Unwin, p. 402.
- Nisbet, E.G., Wilson, J.F., Bickle, M.J., 1981. The evolution of the Rhodesian craton and adjacent Archaean terrain: tectonic models. In: Kroner, A. (Ed.), *Precambrian Plate Tectonics*, Elsevier, p. 161–183.
- Nisbet, E.G., Bickle, M.J., Orpen, J.L., Martin, A., 1993. Controls on the formation of the Belingwe Greenstone Belt, Zimbabwe. In: Bickle, M.J., Nisbet, E.G. (Eds.), *The Geology of the Belingwe Greenstone Belt, Zimbabwe: A Study of the Evolution of Archaean Continental Crust*. A.A. Balkema, Rotterdam, pp. 215–223.
- Podmore, F., 1985. A gravity survey of the Great Dyke, Zimbabwe. Unpublished PhD Thesis, University of London, London, p. 450.
- Podmore, F., Wilson, A.H., 1987. A reappraisal of the structure and emplacement of the Great Dyke, Zimbabwe. *Geological Association Canada Special Paper* 33, pp. 317–330.
- Ranganai, R.T., 1985. A gravity study of the Belingwe greenstone belt. Unpublished MSc Thesis, University of Zimbabwe, Harare, p. 100.
- Ranganai, R.T., 1993. Interpretation of aeromagnetic and gravity data of the Belingwe greenstone belt, Zimbabwe. *ITC Journal* 1993-2, 193.
- Ranganai, R.T., 1995. Geophysical Investigations of the Granite-Greenstone Terrain in the South-Central Zimbabwe Archaean craton. PhD Thesis, University of Leeds, Leeds, UK, p. 288.
- Ranganai, R.T., Ebinger, C.J., Whaler, K.A., 1994. Structural geology and regional tectonics of the south-central Zimbabwe craton from aeromagnetic, gravity and LANDSAT TM data. In: 56th EAEG Meeting, Extended Abstract, Paper P007.
- Reeves, C.V., 1989. Geophysical mapping of Precambrian granite-greenstone terrains as an aid to exploration. *Ontario Geological Survey Special* 3, 254–266.
- Ridley, J.R., Kramers, J.D., 1990. The evolution and tectonic consequences of a tonalitic magma layer within Archaean continents. *Canadian Journal Earth Sciences* 27, 218–228.
- Robertson, I.D.M., 1973. Potash Granites of the Southern Edge of the Rhodesian Craton and the Northern Granulite Zone of the Limpopo Belt, vol. 3. Geological Society South Africa Special Publication, pp. 265–276.
- Robertson, I.D.M., 1974. Explanation of the geology south of Chibi. Rhodesia Geological Survey Short Report 41, p. 40.
- Rollinson, H.R., 1993. A terrane interpretation of the Archaean Limpopo Belt. *Geological Magazine* 130, 755–765.
- Rollinson, H.R., Blenkinsop, T., 1995. The magmatic, metamorphic and tectonic evolution of the Northern Marginal Zone of the Limpopo Belt in Zimbabwe. *Journal Geological Society London* 152, 65–75.
- Rudman, A.J., Mead, J., Whaley, J.F., Blakely, R.F., 1971. Geophysical analysis in central Indiana using potential field continuation. *Geophysics* 36, 878–890.
- Schwerdtner, W.M., Stone, D., Osadetz, K., Morgan, J., Scott, G.M., 1979. Granitoid complexes and the Archaean tectonic record in the southern part of northwestern Ontario. *Canadian Journal Earth Sciences* 16, 1965–1977.
- Simpson, R.W., Jachens, R.C., Blakely, R.J., Saltus, R.W., 1986. A new isostatic residual gravity map of the conterminous United States with a discussion on the significance of isostatic residual anomalies. *Journal of Geophysical Research* 91 (B8), 8348–8372.
- Smith, W.H.F., Wesel, P., 1990. Gridding with continuous curvature splines in tension. *Geophysics* 55, 293–305.
- Stettler, E.H., de Beer, J.H., Eberle, D., Ludden, J., Mareschal, M., 1997. Geophysics and deep structures. In: de Wit, M.J., Ashwal, L.D. (Eds.), *Greenstone Belts*, Oxford Monograph on Geology and Geophysics. Clarendon Press, Oxford, pp. 567–580.
- Stuart, G.W., Zengeni, T.G., 1987. Seismic crustal structure of the Limpopo mobile belt, Zimbabwe. *Tectonophysics* 144, 232–335.
- Subrahmanyam, C., Verma, R.K., 1981. Densities and magnetic susceptibilities of precambrian rocks of different metamorphic grade (Southern Indian Shield). *Journal of Geophysics* 49, 101–107.
- Subrahmanyam, C., Verma, R.K., 1982. Gravity interpretation of the Dharwar greenstone-gneiss-granite terrain in the southern Indian Shield and its geological implications. *Tectonophysics* 84, 225–245.
- Szewczyk, Z.J., West, G.F., 1976. Gravity study of an Archaean granitic area north of Ignace, Ontario. *Canadian Journal Earth Sciences* 13, 1119–1130.
- Taylor, P.N., Kramers, D.J., Moorbath, S., Wilson, J.F., Orpen, J.L., Martin, A., 1991. Pb/Pb, Sm–Nd and Rb–Sr geochronology in the Archaean craton of Zimbabwe. *Chemical Geology (Isotopy Geoscience)* 87, 175–196.
- Telford, W.M., Geldart, L.P., Sheriff, R.E., 1990. *Applied Geophysics*, 2nd ed. Cambridge University Press, Cambridge, p. 770.
- Thurston, B.J., Brown, R.J., 1994. Automated source-edge location with a new variable pass-band horizontal gradient operator. *Geophysics* 59, 546–554.
- Treloar, P.J., Blenkinsop, T.G., 1995. Archaean deformation patterns in Zimbabwe: true indicators of Tibetan-style crustal extrusion or not? In: Coward, P., Ries, A.C. (Eds.), *Early Precambrian Processes*, vol. 95. Geological Society Special Publication, pp. 87–108.
- van Reenen, D.D., Roering, C., De Wit, M.J., Barton, J.M., Ashwal, L.D., 1992. The Archaean Limpopo granulite belt: tectonics and deep crustal processes. *Precambrian Research* 55, 1–587.

- Wilson, J.F., 1979. A preliminary reappraisal of the Rhodesian basement complex. *Geological Society South Africa Special Publication* 5, 1–23.
- Wilson, J.F., 1981. The granite-gneiss greenstone shield, Zimbabwe. In: Hunter, D.R. (Ed.), *Precambrian of the Southern Hemisphere*. Elsevier, pp. 454–488.
- Wilson, J.F., 1990. A craton and its cracks: some of the behaviour of the Zimbabwe block from the Late Archaean to the Mesozoic in response to horizontal movements, and the significance of some of its mafic dyke fracture patterns. *Journal African Earth Sciences* 10, 483–501.
- Wilson, J.F., Bickle, M.J., Hawkesworth, C.J., Martin, A., Nisbet, E.G., Orpen, J.L., 1978. The granite-greenstone terrains of the Rhodesian Archaean craton. *Nature* 271, 23–27.
- Wilson, J.F., Jones, D.L., Kramers, J.D. 1987. Mafic dyke swarms in Zimbabwe. In: Halls, H.C., Fahrig, W.F. (Eds.), *Mafic Dyke Swarms*, Geological Association Canada Special Paper 33, pp. 433–444.
- Wilson, J.F., Nesbitt, R.W., Fanning, C.M., 1995. Zircon geochronology of Archaean felsic sequences in the Zimbabwe craton: a revision of greenstone stratigraphy and a model for crustal growth. In: Coward, M.P., Ries, A.C. (Eds.), *Early Precambrian Processes*, vol. 95. Geological Society Special Publication, pp. 109–126.
- Windley, B.F., 1993. Uniformitarianism today: plate tectonics is the key to the past. *Journal Geological Society London* 150, 7–19.
- Won, I.J., Bevis, M., 1987. Computing the gravitational and magnetic anomalies due to a polygon: algorithms and Fortran subroutines. *Geophysics* 52, 232–238.